Available online at www.sciencedirect.com

ScienceDirect

Procedia Structural Integrity 35 (2022) 228–236

Structural Integrity Procedia

www.elsevier.com/locate/procedia

2nd International Workshop on Plasticity, Damage and Fracture of Engineering Materials

The influence of thickness/grain size ratio in microforming through crystal plasticity

Orhun Bulut[a], Sadik Sefa Acar[a,b], Tuncay Yalçinkaya[a,*]

[a] *Department of Aerospace Engineering, Middle East Technical Universty, Ankara 06800, Turkey*
[b] *Repkon Machine and Tool Industry and Trade Inc., Istanbul 34980, Turkey*

Abstract

Microscale forming operations have become popular due to miniaturisation which focuses on micro scale design and manufacturing of devices, components and parts, e.g. in RF-MEMS. In such processes when the component dimension becomes comparable with the grain size, considerable size effect is observed. Recent experimental studies on micron sized sheet specimens have shown that the ratio between thickness (t) and grain size (d) has a significant influence on the mechanical behavior of materials which cannot be explained merely with the intrinsic (grain) size effect. Even though the grain sizes are similar, remarkable differences in mechanical response is obtained for cases with different thicknesses. In this context the aim of the current study is to address this extrinsic type size effect through crystal plasticity simulations. A series of local crystal plasticity finite element simulations are conducted for different values of t/d ratio in tensile specimens. Different granular morphologies of polycrystalline samples are generated using Voronoi tessellation and tested under axial loading conditions. The macroscopic influence of varying t/d ratio is studied in detail and compared with the experimental findings in the literature.

Keywords: Crystal Plasticity; Size effect; Microforming

1. Introduction

The ongoing technological advancements lead to usage of micron-sized devices necessary in various industries. Because of the popularization of such tiny devices, there is a need for further investigation of the influence of microstructural characteristics on the mechanical response. At this length scale, different size effect phenomena plays crucial role in the plastic behavior of the materials (see e.g. Yalçinkaya et al. (2018)). As the material become thinner, fewer grains are present along the thickness direction. Hall-Petch relation dictates that material strength strongly depends on the grain size with an inverse relation, which assumes a certain dependency for every grain size independent of the specimen geometry. However, this traditional perspective of the grain size effect is not enough to explain the

* Corresponding author. Tel.: +903122104258 ; fax: +903122104250.
E-mail address: yalcinka@metu.edu.tr

10.1016/j.prostr.2021.12.069

mechanical behaviour of specimens with few grains per thickness (see e.g. Kim and Lee (2012)). Experimental studies have shown that thickness to grain size ratio (t/d) is a significant factor on the account of mechanical behavior (see e.g. Janssen et al. (2006); Hug and Keller (2010); Keller et al. (2011)). In these experimental studies, the thickness to grains size ratio (t/d) is controlled by either keeping the thickness constant and changing the grain size (by heat treatment) or preserving the same grain size for different thickness values. Variation in mechanical responses is observed among these specimens. Flow stress decreases with decreasing thickness to grain size ratio (t/d) much more drastically for thin specimens in a certain interval. So in this interval, thin materials follow a different trend from the bulk specimens in terms of flow stress and show a "multicrystalline behavior", see region B in Fig. 1. The value of t/d below which specimens follow this trend, is called critical value. The critical value differs for each material. After that critical value, material behave like a "polycrystal", see region C in Fig. 1. Moreover, for specimens having less than one grain per thickness which is called "monocrystals", similiar values of flow stress are recorded, see region A in Fig. 1. This is due to the fact that surface grain ratio stays constant for all specimens, since all the grains are surface grains.

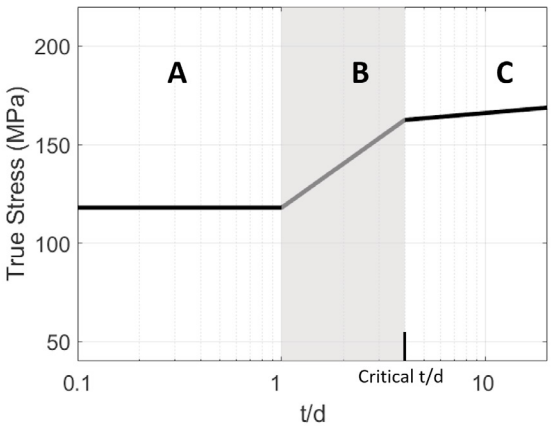

Fig. 1: Experimental true stresses for different t/d ratios of nickel at 0.05 strain presented in Hug and Keller (2010).

As fewer grains are present along the thickness direction, the ratio of grains having at least one free surface increases. Therefore, surface grains become more and more dominant on the specimen which leads to inferior mechanical properties (see e.g. Miyazaki et al. (1979)). The main reason is that the inner grains are much more constrained by the neighbouring grains than surface grains leading to more dislocation grain boundary interaction and more hardening. The exponential decrease of flow stress with the decrease of t/d is explained by this proportional increase of free surface (see e.g. Kals and Eckstein (2000); Raulea et al. (2001); Janssen et al. (2006); Keller et al. (2010)). Moreover, low t/d ratio might lead to an anisotropic behavior since each grain will possess a strong influence on the overall behavior. Besides anisotropy, the grain boundaries are also crucial in these specimens which can be grouped as vertical GB (along thickness direction) and horizontal GB (along the loading direction). For t/d values below 1, only vertical GBs are present since all grains become columnar. However, for t/d values higher than 1, grains start to stack on each other and horizontal GBs come into action. As the t/d is further increased until the critical value, the amount of the horizontal grain boundaries increases significantly, which can be regarded as one of the factors that ensures the increase in flow stress in the interval before the critical value (see e.g. Janssen et al. (2006); Hug and Keller (2010)).

The effect of the thickness to grain size ratio on flow stress is observed experimentally as explained above. In this paper, the phenomena is studied numerically with crystal plasticity finite element method. A local crystal plasticity model is employed to assess the mechanical behavior of thin materials. A representative volume element with 300 grains is created and parameters for the model are fitted to the experimental data of the aluminum AA6016 in T4 temper. Specimens with varying t/d ratios are created and subjected to the uniaxial tensile loading simulations. The obtained results are compared with experimental studies and the capacity of crystal plasticity finite element calculations is discussed in this context.

2. Constitutive Model

A rate-dependent finite strain local crystal plasticity model with hardening law of Peirce et al. (1982) is employed within the finite element analyses in this study. Crystallographic slip due to dislocation motion on active slip systems and elastic lattice distortion are the two main mechanisms that cause the entire deformation. The deformation gradient $\mathbf{F}$ is decomposed in a multiplicative manner,

$$\mathbf{F} = \mathbf{F}^e \cdot \mathbf{F}^p \tag{1}$$

where $\mathbf{F}^e$ and $\mathbf{F}^p$ are the elastic and plastic deformation gradient, respectively. $\mathbf{F}^e$ is related to the stretching and rotation of the crystal lattice. Plastic deformation is assumed to be occurred only due to the crystalline slip. Thus, $\mathbf{F}^p$ includes only the effect of plastic shear,

$$\mathbf{L} = \dot{\mathbf{F}} \cdot \mathbf{F}^{-1} = \mathbf{D} + \mathbf{\Omega} \tag{2}$$

Total velocity gradient $\mathbf{L}$ actually consists of the symmetric rate of stretching $\mathbf{D}$ and the antisymmetric spin tensor $\mathbf{\Omega}$. Then $\mathbf{D}$ and $\mathbf{\Omega}$ are additively decomposed to elastic and plastic parts,

$$\mathbf{D} = \mathbf{D}^e + \mathbf{D}^p \ , \quad \mathbf{\Omega} = \mathbf{\Omega}^e + \mathbf{\Omega}^p \tag{3}$$

The plastic deformation gradient is determined by integrating the plastic velocity gradient, which is obtained by summing the plastic slip rate $\dot{\gamma}$ on each slip system,

$$\mathbf{L}_p = \dot{\mathbf{F}} \cdot (\mathbf{F}^p)^{-1} = \sum_{\alpha=1}^{N} \dot{\gamma}^{(\alpha)} (\mathbf{m}^{(\alpha)} \otimes \mathbf{n}^{(\alpha)}) \tag{4}$$

where $\mathbf{m}^\alpha$ and $\mathbf{n}^\alpha$ represent the slip direction and the normal to the slip plane of the slip system α. The evolution of the slip rate $\dot{\gamma}$ occurs according to the power law shown below,

$$\dot{\gamma}^{(\alpha)} = \dot{\gamma}_0 \left| \frac{\tau^{(\alpha)}}{g^{(\alpha)}} \right|^n \text{sign}(\tau^{(\alpha)}). \tag{5}$$

where $\dot{\gamma}_0$ denotes reference plastic slip rate and n represents the rate sensitivity exponent. $\tau^{(\alpha)}$ and $g^{(\alpha)}$ denote resolved shear stress and slip resistance, respectively. The slip resistance evolves according to

$$\dot{g}^{(\alpha)} = \sum_{\beta} h^{\alpha\beta} \left| \dot{\gamma}^{\beta} \right| \tag{6}$$

For self-hardening Peirce and Asaro's (sech) relation is employed,

$$h^{\alpha\alpha} = h(\gamma) = h_0 \text{sech}^2 \left| \frac{h_0 \gamma}{g_s - g_0} \right| \tag{7}$$

where h_0 is the initial hardening modulus, g_0 is the initial slip resistance, g_s is the saturation slip resistance. Latent hardening moduli are given by

$$h^{\alpha\beta} = q^{\alpha\beta} h^{\alpha\alpha} \ , \quad (\alpha \neq \beta) \tag{8}$$

where q denotes the ratio of latent hardening to self-hardening. All 12 slip systems are included for the FCC (Face Centered Cubic) material which are assumed to be active.

3. Numerical study

In this section the numerical analysis of specimens with different thickness/grain size ratio is presented. After identifying the material parameters through a homogenization process various cases are studied and the results are discussed in comparison to experimental observations from the literature.

3.1. Material parameters

The crystal plasticity finite element simulations are conducted in ABAQUS employing a user-material subroutine (UMAT) based on Huang (1991) with certain modifications. For the identification of material parameters an artificial representative volume element (RVE) is generated through Voronoi tessellation using Neper software with 300 grains (see Quey et al. (2011)). The material data for AA6016 in T4 temper condition is considered (Granum et al. (2019)) and the stress-strain response is fitted to the ones from the RVE computations. Symmetric boundary conditions with tensile loading are imposed such that all surfaces of RVE are kept straight and ensure that triaxiality values remain 0.33 (see e.g. Yalçinkaya et al. (2021a)).

Cubic elastic parameters for aluminum sheet is taken as $C_{11} = 108.2$ GPa, $C_{12} = 61.3$ GPa and $C_{44} = 28.5$ GPa (Nakamachi et al. (2002)). Reference slip rate $\dot{\gamma}_0$ is taken as 10^{-3} and rate sensitivity exponent n is determined as 60 for analyses to be rate-independent as much as possible. The ratio of latent hardening to self-hardening q is a constant for all grains and taken as 1.4 considering strong latent hardening for aluminum (see e.g. Peirce et al. (1982); Liu et al. (2019)). After the identification process, the hardening parameters are obtained as, initial hardening modulus $h_0 = 190$ MPa, saturation slip resistance $g_s = 95$ MPa and initial slip resistance $g_0 = 47$ MPa. Additionaly, three different simulations with different sets of random orientations are conducted to verify the obtained hardening parameters, see Fig. 2. For both parametrization and main analyses, the strain rate is determined as 10^{-3}.

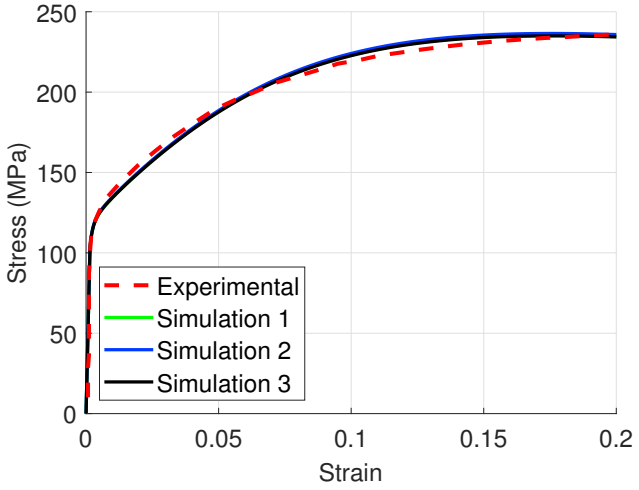

Fig. 2: Experimental versus RVE stress strain response under axial loading condition for three different randomly oriented grain microstructures.

3.2. Tensile specimens

Tensile specimens are generated with 2 mm x 2 mm dimensions having varying thicknesses, see Table 1. Four example microstructures of the specimens are presented in Fig. 3. Grain orientations are assigned randomly for each grain where Euler ZYX convention is followed. The intervals for Euler angles are selected as ϕ[0 360], θ[0 180],ψ[0 360].

Boundary conditions are visualized in Fig. 4. All the nodes of the bottom surface are constrained in Y direction while the node at the origin is constrained in all three axial directions. Moreover, x1 node is constrained in z-direction while z1 node is constrained in the x-direction to eliminate any possible rigid body rotation and ensure uniaxial tension.

The employed local plasticity cannot predict the intrinsic size effect due to varying grain size. In order to include such effects a strain gradient crystal plasticity model should be used (see e.g. Yalçinkaya (2019), Yalçinkaya et al. (2021b), Yalçinkaya et al. (2021c)). The variation of both grain size and the thickness makes the analysis complicated and it would be difficult to get a clear conclusion when both intrinsic and extrinsic size effect is active. Therefore as an initial attempt we keep the grain size around a constant value and vary the thickness using a size-independent model.

Table 1: Dimensions and corresponding t/d ratios of examined specimens.

x dimension (mm)	y dimension (mm)	thickness (μm)	mean grain diameter (μm)	t/d ratio	total number of grains
2	2	18	59	0.30	665
2	2	35	73	0.48	665
2	2	53	85	0.62	665
2	2	70	93	0.75	665
2	2	88	100	0.88	665
2	2	105	105	1	685
2	2	147	105	1.4	959
2	2	168	105	1.6	1096
2	2	189	105	1.8	1233
2	2	211	105	2	1370
2	2	232	105	2.2	1507
2	2	253	105	2.4	1644
2	2	274	105	2.6	1781
2	2	295	105	2.8	1918
2	2	316	105	3	2055
2	2	358	105	3.4	2329
2	2	400	105	3.8	2603
2	2	442	105	4.2	2877
2	2	484	105	4.6	3151
2	2	526	105	5	3425
2	2	568	105	5.4	3699

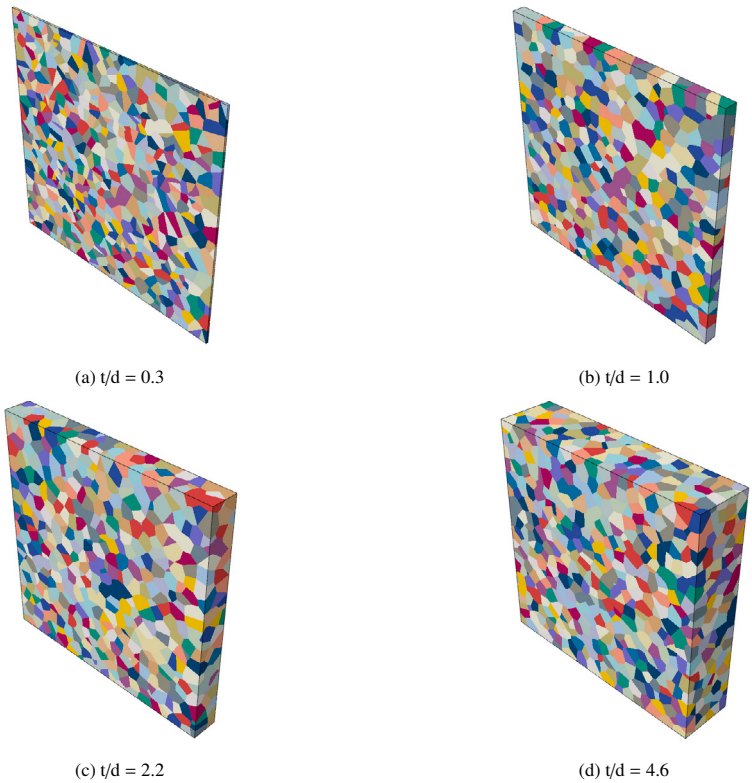

(a) t/d = 0.3 (b) t/d = 1.0

(c) t/d = 2.2 (d) t/d = 4.6

Fig. 3: Microstructures of specimens having different t/d values.

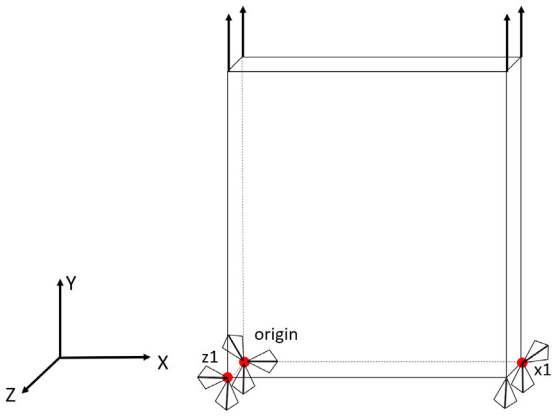

Fig. 4: Boundary condition for uniaxial tension simulation.

In this way the hardening parameters are naturally kept constant in all simulations. The strategy of controlling the t/d ratio by changing thickness is also conducted experimentally in literature (see e.g. Hug and Keller (2010); Yuan et al. (2020)). Note that the CPFE model does not include the effect of grain boundaries directly. For a more physical analysis where the influence of grain boundary orientation and the misorientation between the grains are considered, a proper GB model should be included in the modeling (see e.g. Yalçinkaya et al. (2021b)). In here the misorientation between the neighbouring grains create a constraining effect anyhow due to the different plasticity evolution coming from the random orientation distribution. Therefore, the model indirectly considers the effect of the grain boundaries with a limited capacity.

A mean grain size of 105 μm is considered for each specimen with t/d > 1. The thickness of the specimens vary between 18 μm and 568 μm, which leads to t/d ratios within an interval between 0.3 and 5.4. To capture the critical value of the t/d ratio, the thickness is gradually increased until the increase in flow stress is almost levelled off. In order to preserve the mean grain size, the number of grains is increased from 685 (t/d=1.0) to 3699 (t/d=5.4) by increasing the thickness. On the other hand, the specimens having t/d ratio below 1 consist of 665 grains.

4. Results

In the simulations, a general trend of increase in flow stress with increasing t/d ratio is observed, which is obtained solely through thickness increase. In this analysis the number of grains should be increased to see the influence of higher t/d ratios. Even though the total grain number is increased, the number of grains at the free surfaces stays nearly constant for all t/d ratios. Therefore, the ratio of the surface grains to all grains decreases for increasing t/d. As discussed previously, higher the surface grain ratio weaker the stress response. The results presented in Fig. 5 confirm this simple relation where the flow stress increases with increasing t/d and with decreasing surface grain ratio. At t/d equals 1, almost all grains are surface grains and the stress response is lowest among the other specimens having higher t/d. In Fig. 5a, it can be observed that flow stress increases rapidly with increasing t/d but then the rate of increase slows down. Fig. 5b shows that the increasing trend in flow stress diminishes for higher t/d ratios and the results converge to a single curve, which is expected for a polycrystalline material.

To get a better comparison with the experimental behavior shown in Fig. 1, the flow stress values at 0.1 macroscopic strain are plotted for different specimens with different t/d values in Fig. 6. In the experimental studies, flow stresses do not change much for specimens with t/d < 1. When the ratio is increased further until the critical value, flow stresses are observed to be increasing rapidly. Above the critical value, the increase slows down and similar flow stress values are recorded for higher t/d ratios. In the current numerical study, the most obvious difference with experiments is obtained for t/d < 1 where a considerable increase in flow stresses occur. One of the reasons is that, in our simulations, the imposed boundary conditions make the specimen deform homogeneously, therefore it delays the localization. Another reason is that, even though the surface grain ratios are similar, the amount of grain boundaries

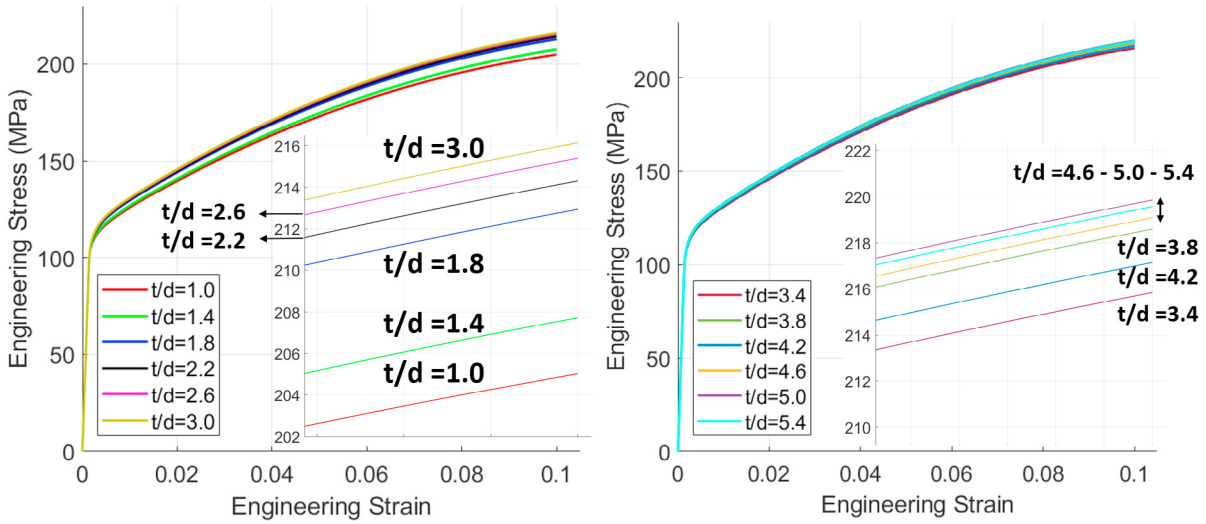

(a) Engineering stress-engineering strain curves of specimens having t/d below 3 (b) Engineering stress-engineering strain curves of specimens having t/d above 3

Fig. 5: Engineering stress-engineering strain curves for specimens having different t/d ratios.

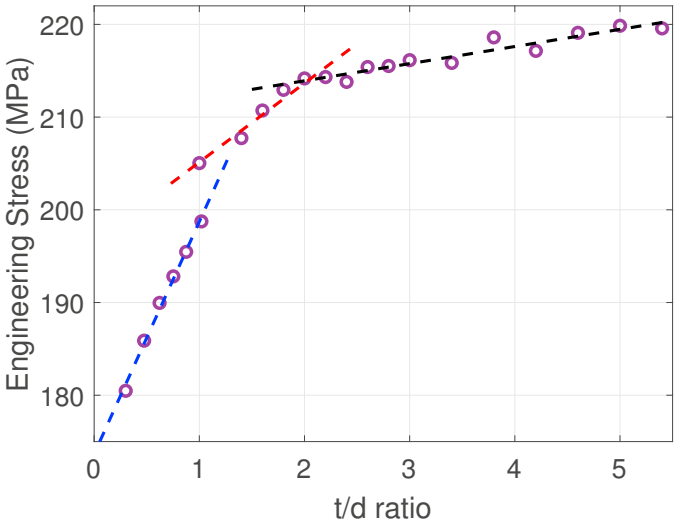

Fig. 6: Flow stress values at %10 displacement of specimens having different t/d ratios.

changes dramatically for these specimens. Moreover, the most important reason is that in the calculations the same hardening parameters are used for each specimen. Yet, while specimens with t/d > 1 have the same mean grain size, the specimens with t/d < 1 show decreasing grain size behavior with decreasing t/d ratio. If hardening parameters were adjusted according to the grain sizes, or if a size dependent crystal plasticity model was employed, which would lead to a harder response, then the results would be similar for t/d < 1 to the experimental observations.

The flow stress response shows a steep increase for t/d between 1 and a critical value compared to the response at higher t/d ratios which converge to polycrystalline behavior. Fig. 6 shows that the critical value corresponds to around 2. Between 1 and the critical value, the numerical study resulted in a similar trend with the experimental results. Starting from t/d = 1, as the ratio is increased, the grain boundaries parallel to the loading direction start to emerge. These GBs contribute to the resistance of the material to plastic deformation. The difference between

flow stresses is not high compared to the experimental studies. The main reason is that the local crystal plasticity method does not include the effect of the grain boundaries directly as it was explained in the simulations section. Yet, there is a distinguishable evolution that constitutes observable trends. The influence of the boundary conditions which leads to same homogeneous behavior in all specimens could influence the difference between the experiments and the numerical results. While in experimental studies the thinner specimens start to localize earlier, here there is no difference in that regard due to homogeneous behavior. As stated previously, the increase in flow stress diminishes after the critical value. The findings of the simulations are parallel to the experiments. For these specimens, at least 2 grains are present through thickness and all grains have at least one horizontal grain boundary. Therefore, newly formed grain boundaries do not create a significant difference in flow stress. As the t/d ratio further exceeds the critical value, the mechanical response approaches to that of the bulk specimen and the effect of having few grains per thickness disappears.

The von Mises stress distributions of specimens with different t/d ratios are shown in Fig. 7. The difference in stress distribution is apparent especially on the lateral (thickness) surface. As the t/d ratio increases, a general increase in the von Mises stress values is apparent. The emergence of new GBs can be observed by examining the stress variation along the upper and lateral surfaces.

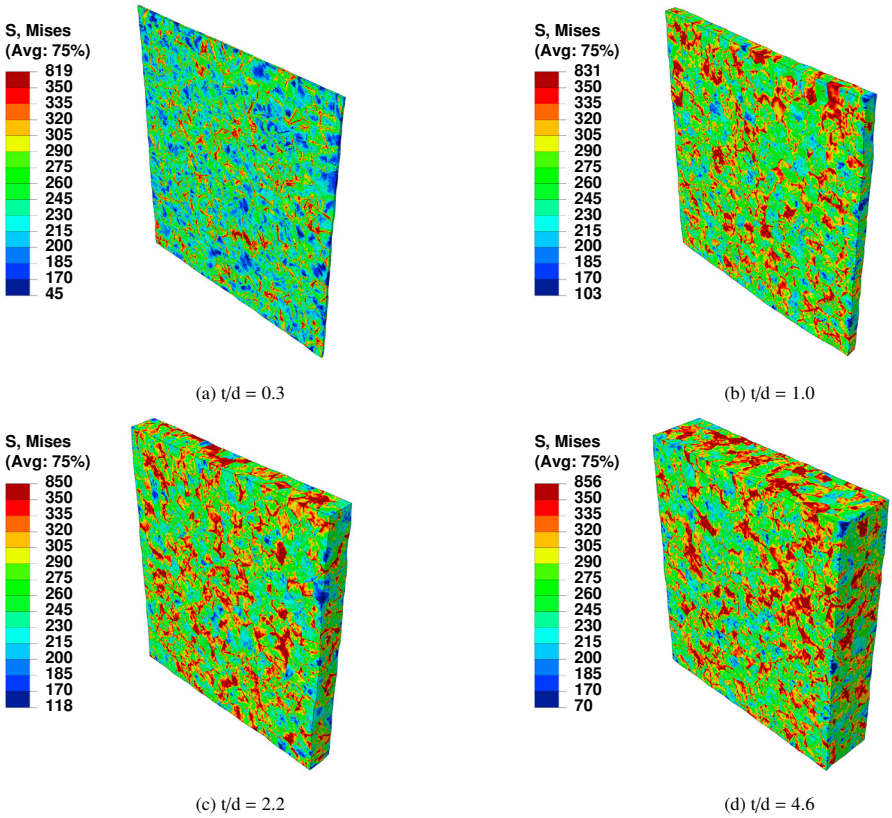

(a) t/d = 0.3 (b) t/d = 1.0

(c) t/d = 2.2 (d) t/d = 4.6

Fig. 7: Von Mises stress distribution of specimens having different t/d ratios.

5. Conclusion

In this paper, the crystal plasticity finite element method is employed to assess the mechanical response of specimens with micron sized thickness having few grains per thickness. A parameter fitting study was conducted at RVE scale to find hardening parameters of AA6016 in T4 temper condition. With obtained hardening parameters, uniaxial tension loading simulations are conducted on thin specimens having different thickness to grain size ratios.

The macroscopic responses of specimens are compared with the experimental findings in the literature in a qualitative manner. For specimens with thickness to grain size ratio t/d < 1, the numerical results were not in an agreement

with the experiments. Significant differences between flow stresses of the specimens were observed even though similar values were recorded in experimental studies. The disagreement was partly due to the boundary conditions which delayed the localization and the variation in the amount of GBs transverse to the loading direction. The most important reason was the same hardening parameters being used for specimens with different mean grain sizes, which would naturally decrease in the t/d < 1 regime. A more accurate study can be conducted in the future with appropriate hardening parameters or by employing a strain gradient crystal plasticity model which would take into account the size effect.

For t/d > 1, flow stresses increase rapidly until the critical value. The critical value is found to be approximately 2. The rapid increase was a result of the development of the GBs parallel to the loading direction. The trend is in line with the empirical tests in literature, yet the differences between flow stresses were lower in simulations compared to the experiments due to the employed local crystal plasticity model which cannot include the direct effect of the GBs as well as the employed homogeneous boundary conditions. Further increase in the t/d ratio, above the critical value, slows down the increase in flow stress. Since there is already a considerable amount of GBs parallel to the loading direction, newly formed GBs do not make a substantial contribution to the resistance to deformation. Also, for specimens with higher t/d ratios, the specimens can no longer be treated as thin specimens and the behavior converges to the polycrystalline one.

References

Granum, H., Aune, V., Børvik, T., Hopperstad, O., S., 2019. Effect of heat-treatment on the structural response of blast-loaded aluminium plates with pre-cut slits. International Journal of Impact Engineering , 103306.

Huang, Y., 1991. A user-material subroutine incroporating single crystal plasticity in the abaqus finite element program. Mech Report 178.

Hug, E., Keller, C., 2010. Intrinsic Effects due to the Reduction of Thickness on the Mechanical Behavior of Nickel Polycrystals. Metallurgical and Materials Transactions: A 41, 2498–2506.

Janssen, P., J., M., Keijser, Th., H., Geers, M., 2006. An experimental assessment of grain size effects in the uniaxial straining of thin al sheet with a few grains across the thickness. Materials Science and Engineering: A 419, 238–248.

Kals, T., A., Eckstein, R., 2000. Miniaturization in sheet metal working. Journal of Materials Processing Technology 103, 95–101.

Keller, C., Hug, E., Retoux, R., Xavier, F., 2010. TEM study of dislocation patterns in near-surface and core regions of deformed nickel polycrystals with few grains across the cross section. Mechanics of Materials 42, 44–54.

Keller, C., Hug, E., Xavier, F., 2011. Microstructural size effects on mechanical properties of high purity nickel. International Journal of Plasticity 27, 635–654.

Kim, H., Lee, Y., 2012. Size dependence of flow stress and plastic behaviour in microforming of polycrystalline metallic materials. Proceedings of the Institution of Mechanical Engineers, Part C: Journal of Mechanical Engineering Science 226, 403–412.

Liu, W., Chen, B., Pang, Y., 2019. Numerical investigation of evolution of earing, anisotropic yield and plastic potentials in cold rolled fcc aluminium alloy based on the crystallographic texture measurements. European Journal of Mechanics - A/Solids 75, 41–55.

Miyazaki, S., Shibata, K., Fujita, H., 1979. Effect of specimen thickness on mechanical properties of polycrystalline aggregates with various grain sizes. Acta Metallurgica 27, 855–862.

Nakamachi, E., Xie, C., Morimoto, H., Morita, K., Yokoyama, N., 2002. Formability assessment of FCC aluminum alloy sheet by using elastic/crystalline viscoplastic finite element analysis. International Journal of Plasticity 18, 617–632.

Peirce, D., Asaro, R., J., Needleman, A., 1982. An Analysis of Nonuniform and Localized Deformation in Ductile Single Crystals. Acta Metallurgica 30, 1087–1119.

Quey, R., Dawson, P., Barbe, F., 2011. Large-scale 3D random polycrystals for the finite element method: Generation, meshing and remeshing. Computer Methods in Applied Mechanics and Engineering 200, 1729–1745.

Raulea, L., V., Goijaets, A., M., Govaert, L., E., Baaijens, F., P., T., 2001. Size effects in the processing of thin metal sheets. Journal of Materials Processing Technology 115, 44–48.

Yalçinkaya, T., 2019. Strain gradient crystal plasticity: Thermodynamics and implementation. Handbook of Nonlocal Continuum Mechanics for Materials and Structures , 1001–1033.

Yalçinkaya, T., Çakmak, S.O., Tekoğlu, C., 2021a. A crystal plasticity based finite element framework for RVE calculations of two-phase materials: Void nucleation in dual-phase steels. Finite Elements in Analysis and Design 187, 103510.

Yalçinkaya, T., Özdemir, İ., Simonovski, I., 2018. Micromechanical modeling of intrinsic and specimen size effects in microforming. International Journal of Material Forming 11, 729–741.

Yalçinkaya, T., Özdemir, İ., Tandoğan, İ., T., 2021b. Misorientation and grain boundary orientation dependent grain boundary response in polycrystalline plasticity. Computational Mechanics 67, 937–954.

Yalçinkaya, T., Tandoğan, İ..T., Özdemir, İ., 2021c. Void growth based inter-granular ductile fracture in strain gradient polycrystalline plasticity. International Journal of Plasticity 147, 103123.

Yuan, Z., Tu, Y., Yuan, T., Zhang, Y., Huang, Y., 2020. Size effects on mechanical properties of pure industrial aluminum sheet for micro/meso scale plastic deformation: Experiment and modeling. Journal of Alloys and Compounds 859, 157752.